

Available at www.sciencedirect.com

SciVerse ScienceDirect

journal homepage: www.elsevier.com/locate/carbon

A green approach for the reduction of graphene oxide by wild carrot root

Tapas Kuila ^a, Saswata Bose ^a, Partha Khanra ^a, Ananta Kumar Mishra ^b,
Nam Hoon Kim ^c, Joong Hee Lee ^{a,b,c,*}

^a WCU Program, Department of BIN Fusion Technology, Chonbuk National University, Jeonju, Jeonbuk 561-756, Republic of Korea

^b BIN Fusion Research Team, Department of Polymer & Nano Engineering, Chonbuk National University, Jeonju, Jeonbuk 561-756, Republic of Korea

^c Department of Hydrogen and Fuel Cell Engineering, Chonbuk National University, Jeonju, Jeonbuk 561-756, Republic of Korea

ARTICLE INFO

Article history:

Received 6 June 2011

Accepted 24 September 2011

Available online 5 October 2011

ABSTRACT

A green approach for the reduction of graphene oxide (GO) using wild carrot root is reported in this work. It avoids the use of toxic and environmentally harmful reducing agents commonly used in the chemical reduction of GO to obtain graphene. The endophytic microorganisms present in the carrot root, reduces exfoliated GO to graphene at room temperature in an aqueous medium. Transmission electron microscopy and atomic force microscopy images provide clear evidence for the formation of few layer graphene. Characterization of the resulting carrot reduced GO by Fourier transform infrared spectroscopy and X-ray photoelectron spectroscopy shows partial reduction of GO to graphene. Raman spectroscopy data also indicates the partial removal of oxygen-containing functional groups from the surface of GO and formation of graphene with defects.

© 2011 Elsevier Ltd. All rights reserved.

1. Introduction

The unique electronic, optical, mechanical, and catalytic properties of graphene, the thinnest known material, have led the development of new areas of nanoscience and technology [1–5]. The excellent characteristics of graphene have opened a new possibility of its application in many electronic devices, such as touch panels, p–n junction materials, flexible thin-film transistors, and solar cells [4–8]. In order to harness these aspects, large scale production of graphene is required. Several methods like chemical vapor deposition (CVD), epitaxial growth on electrically insulating surfaces, electric arc discharge, and solution-based chemical reduction of GO have been reported for the preparation of graphene [9–12]. Among these reported methods, the solution-based reduction of GO possess the advantageous features in terms of cost

effectiveness and bulk-scale productivity [12]. However, the strong tendency of π – π stacking between the chemically reduced GO sheets leads to the formation of irreversible agglomerates. Surface modification of GO using small organic molecules, biomolecules, and polymers can effectively eliminate the afore-mentioned problem [13–16]. However, the use of surface modifiers is problematic as they tend to reduce the electrical conductivity of graphene due to their intrinsic insulating effect, which in turn limits the practical applicability of the surface-modified graphene in the field of nano-electronics. Another drawback is the toxic nature of the chemical reducing agents (hydrazine, hydroquinone, sodium borohydride), which are harmful to the environment. Metal particles may remain as impurities after the metal/hydrochloric acid reduction of GO. Reduction of GO by nontoxic methodologies involves reducing agents having the disadvantages like,

* Corresponding author at: WCU Program, Department of BIN Fusion Technology, Chonbuk National University, Jeonju, Jeonbuk 561-756, Republic of Korea. Fax: +82 63 270 2341.

E-mail address: jhl@chonbuk.ac.kr (J.H. Lee).

0008-6223/\$ - see front matter © 2011 Elsevier Ltd. All rights reserved.

doi:10.1016/j.carbon.2011.09.053

non-availability, limited storage stability, and cost effectiveness [17–21]. Consequently, new approaches need to be explored for the effective conversion of GO into graphene sheets under mild conditions and by utilizing environmentally friendly reducing agents. Wild carrot root has been used extensively for the reduction of aliphatic and aromatic ketones, cyclic ketones, β -keto esters, and azidoketones [22–25]. The endophytic microorganisms present in the carrot root are responsible for carrying out the reduction of organic functional groups [25]. GO sheets are heavily oxygenated, bearing hydroxyl, epoxide, diol, ketone and carboxyl functional groups [16,26]. Therefore, microorganisms in carrots are expected to remove oxygen functionalities from the surface of GO and restore electronic conjugation in graphene. The mild reductive ability of carrots will help to prevent the extensive agglomeration of graphene into graphitic structures. This work reports the simple reduction of GO sheets by using carrots in aqueous solution at room temperature. Most significantly, in comparison with other strong reducing agents used in GO reduction, carrots are readily available and have low environmental impact.

2. Experimental

2.1. Chemicals

Natural graphite flakes (Sigma–Aldrich, Steinheim, Germany) were used as received. Sulfuric acid, hydrochloric acid, and hydrogen peroxide were purchased from Samchun Pure Chemical Co. Ltd. (Pyeongtaek-si, Korea). Potassium permanganate (Junsei Chemical Co. Ltd., City, Japan) was used as an oxidizing agent. Carrots were obtained from a market in Jeonju, Korea. The bacterial inhibitors (chloramphenicol and cycloheximide) were purchased from Sigma–Aldrich and used without further purification.

2.2. Synthesis of GO

GO was synthesized from natural graphite by following a modified Hummers method [27]. In brief, 2 g of natural graphite flake was dispersed in 46 ml of concentrated sulfuric acid in an ice bath. About 6 g of potassium permanganate was slowly added for 15–20 min at 0–5 °C and stirring was continued for 2 h. The reaction mixture was subsequently transferred to a pre-heated oil bath at 35 °C and stirred overnight. Ninety-two milliliters of de-ionized (DI) water was carefully added to the reaction mixture and stirring was continued for another 2 h. The reaction mixture was then transferred to a 1 l beaker and 35% hydrogen peroxide solution was added drop wise until the color of the solution became bright yellow. Dilute hydrochloric acid solution (5% by volume) was added to remove excess of manganese salt. As-synthesized GO was dispersed in water, resulting in the formation of brown dispersion. The dispersed GO was repeatedly washed with DI water to completely remove the residual salts and acids. The purified GO was finally dispersed in water (0.5 mg/ml) and ultrasonically exfoliated in an ultrasonic bath (Sonosmasher ULH 700S, 20 kHz). The dispersion was found to be stable for a long time.

2.3. Reduction of GO by carrot root

In a typical experiment, carrots were washed under tap water and subsequently with DI water. The carrots were peeled and thinly sliced (ca. 1 cm long) for improved contact between the GO and biocatalyst in the carrots. About 5 g of sliced carrot was added to 200 ml of GO dispersion (0.5 mg/ml) at room temperature (25 °C). The reaction mixtures were magnetically stirred (150 rpm) at room temperature for various time. After stirring at room temperature for 48 h the carrot roots were carefully separated followed by refluxing the GO dispersion for 24 h. Table 1 lists the experimental conditions used in each case to obtain different carrot reduced GO (CR-GO).

2.4. Controlled experiment

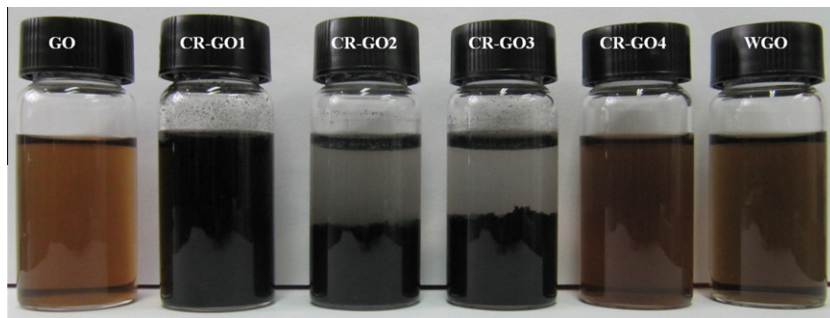
In order to ensure the reduction of GO by wild carrot root, control experiment was carried out in DI water. The GO dispersion (0.5 mg/ml) was refluxed at 100 °C for 24 h. It was found that the color of the GO dispersion (WGO) remained unchanged. This indicated that the wild carrot root played an important role in the reduction of GO to graphene. Another control experiment was carried out to confirm the reduction of GO by the endophytic microorganisms in wild carrot root. For this, bacterial inhibitors (chloramphenicol and cycloheximide), and carrot roots were added to 200 ml GO dispersion (0.5 mg/ml) and stirred for 48 h at room temperature. It was found that the color of the GO dispersion remained unchanged and no phase separation of GO with water was observed. Hydrazine reduction of GO was carried out to compare the quality of CR-GOs to that of the hydrazine reduced GO (HR-GO). For this, 0.5 ml of hydrazine monohydrate was added to 200 ml of GO dispersion (0.5 mg/ml) and was refluxed at 100 °C for 24 h. Fig. 1 shows the digital photograph of different samples to confirm the reduction of GO by wild carrot root. The photographs reveal that there was almost no difference in color of the CR-GO4 and WGO when compared to the aqueous dispersion of pure GO.

2.5. Characterization

X-ray diffraction (XRD) studies were carried out at room temperature on a D/Max 2500V/PC (Rigaku Corporation, Tokyo, Japan) at a scan rate of 1°/min. Fourier transform infrared spectroscopy (FT-IR) was performed over the wave number range of 4000–400 cm^{-1} by using a Nicolet 6700 spectrometer (ThermoScientific, USA). Raman spectra of pure GO, CR-GOs, and HR-GO were obtained on a Nanofinder 30 (Tokyo Instruments Co., Osaka, Japan). GO, CR-GOs, and pure graphite were characterized by X-ray photoelectron spectroscopy (XPS) (Axis-Nova, Kratos Analytical Ltd., Manchester, UK) by using an unmonochromated Al-K α X-ray source (1486.6 eV). The pass energy of the hemisphere analyzer was set at 40 eV for narrow scan and at 160 eV for wide scan. The base pressure and dwell time were 5.2×10^{-9} torr and 100 ms, respectively. The XPS spectrum of GO and CR-GOs remaining after peak separation and background subtraction was compared to that obtained after subtraction of a Shirley background followed by curve fitting of the substrate contribution. The photoionization cross sections for carbon

Table 1 – Preparative conditions and designation of different CR-GOs.

Sample name	Weight of GO (mg)	Volume of water (ml)	Weight of carrot root (g)	Weight of inhibitors (mg)	Stirring at room temperature (h)	Refluxing time (h)
CR-GO1	100	200	5	–	48	–
CR-GO2	100	200	5	–	72	–
CR-GO3	100	200	5	–	48	24
CR-GO4	100	200	5	50 + 50	48	–
WGO	100	200	–	–	–	24

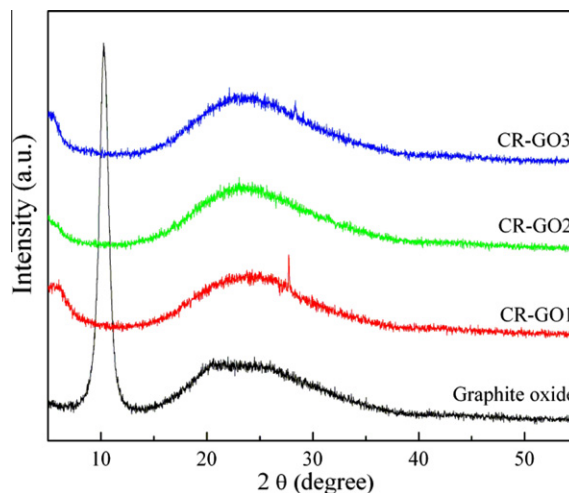
**Fig. 1 – Digital photograph of pure GO, CR-GOs, and WGO.**

and oxygen were taken as 0.01367 and 0.04005, respectively. The microstructure of the samples was investigated by transition electron microscopy (TEM, JEOL JEM-2200 FS), and atomic force microscopy (AFM, XE-100, PARK System, Suwon, South Korea). For TEM analysis, CR-GOs were suspended in water (~ 0.2 mg/ml) by ultrasonication for 15 min and then the unstable dispersion was drop casted on a fresh lacey carbon TEM grid. The beam energy used for TEM analysis was 200 keV. Thermogravimetric analysis (TGA) was carried out on a Q50 TGA (TA instruments, New Castle, Delaware, USA), at a heating rate of 5 °C/min from 60 to 700 °C in nitrogen.

3. Results and discussion

3.1. XRD analysis

X-ray diffraction (XRD) patterns of graphite oxide, CR-GO1, CR-GO2, and CR-GO3 are shown in Fig. 2. Pristine graphite exhibits a basal reflection (002) peak at $2\theta = 26.6^\circ$ (d spacing = 0.335 nm) [28]. Upon oxidation of pristine graphite, the 002 reflection peak shifts to the lower angle ($2\theta = 11.2^\circ$, d spacing = 0.79 nm). The increase in d spacing is due to the intercalation of water molecules and the formation of oxygen-containing functional groups between the layers of the graphite. The XRD of CR-GOs show the appearance of a broad band centered at $2\theta \sim 23.96^\circ$ corresponding to the stacking of graphene layers. The disappearance of 002 reflection peak of graphite oxide and appearance of a broad band at $2\theta \sim 23.96^\circ$ in the CR-GOs indicate the formation of few-layer graphene. However, XRD is not the best tool to identify single-layer graphene. Hence, transmission electron microscopy (TEM) and atomic force microscopy (AFM) were performed for the characterization of graphene.

**Fig. 2 – X-ray diffraction patterns of pure GO and CR-GOs.**

3.2. TEM and AFM analysis

The TEM images of CR-GO2 and CR-GO3 both at lower and higher magnifications are shown in Fig. 3. Appearance of transparent and silky sheets of CR-GO in TEM image corroborates its stability under high energy electron beam. The high-resolution TEM (HR-TEM) image is used to access the number of layers at multiple locations. The edges of the suspended graphene films tend to fold back, allowing cross-sectional view of the films. The folding of one or two layers at the edges of the films appear as one or two dark lines, respectively. HR-TEM images of CR-GO2 and CR-GO3 are shown in Fig. 3e and f. The formation of few layer graphene is clearly visible in the HR-TEM images. The small angle electron diffraction

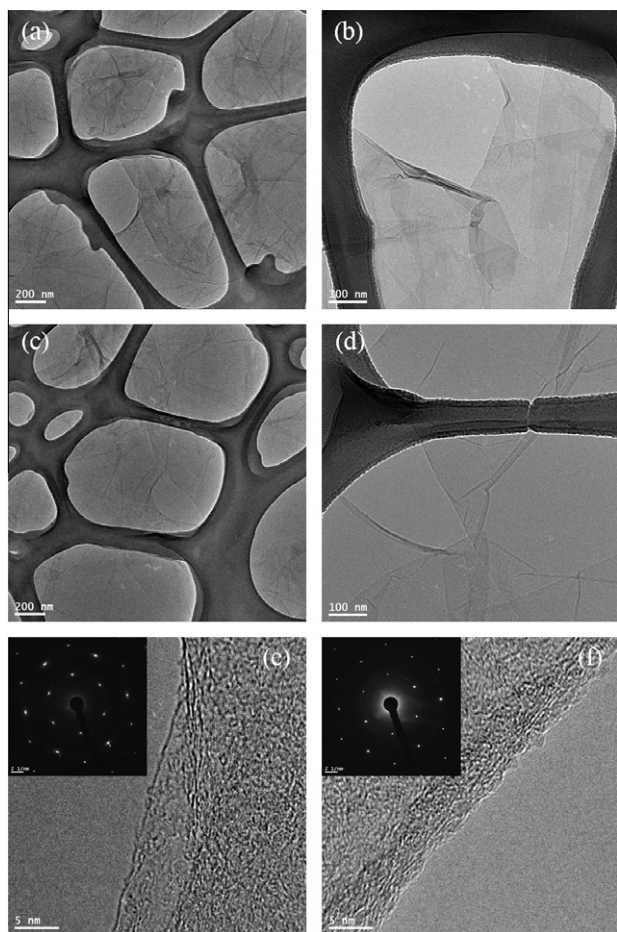


Fig. 3 – TEM images of (a, b) CR-GO2 and (c, d) CR-GO3 at lower and higher magnifications. HR-TEM images of (e) CR-GO2 and (f) CR-GO3 showing the formation of few layer graphene. The SAED pattern (inset of e and f) also supports the formation of few layer graphene.

(SAED) pattern of the CR-GOs reveals a sixfold symmetry as shown in the inset of Fig. 3e and f. It has also been found that the intensities of all the diffraction spots are not equal and sharp enough. Moreover, the diffraction spots are associated with some unresolved spots. All these observations further supporting the formation of few layer graphene [29]. However, this kind of diffraction pattern may also arise from the adsorption of β -carotene (comes from carrot root) on the surface of graphene. Similar kinds of SAED pattern have also been observed for oxidized pyrrole adsorbed few layer graphene [17]. In addition, the broad D and G peaks measured with Raman spectroscopy indicate quite a bit of disorder, which preclude the observation of sharp diffraction spots in the SAED pattern of CR-GOs.

AFM allows definite identification of the number of layers in graphene samples. Fig. 4 shows AFM images of pure GO and CR-GO3, respectively. The average thickness of graphene oxide has been determined to be 1.7 nm, indicating the formations of bi-layer GO. The increased thickness of GO is due to the presence of oxygen functionalities on the graphene sheets. The thickness of CR-GO3 increases to 2.5 nm, which is attributable to the tendency of graphene layers to restack in the absence of stabilizing molecules.

3.3. FT-IR analysis

Fig. 5 shows the Fourier transform infrared (FT-IR) spectra of pure GO and various CR-GO samples. The intensities of the FT-IR peaks corresponding to the oxygen functionalities such as the C=O stretching vibration peak at 1728 cm^{-1} and O-H deformation peak at 1395 cm^{-1} decreases to a significant extent after 72 h reduction of GO by carrot [19]. The intensities of the C–O (epoxy) stretching vibration peak of GO at 1223 cm^{-1} , and the C–O (alkoxy) stretching vibration peak at 1051 cm^{-1} remains almost unchanged; however, the peak positions have changed significantly in the CR-GOs. This is attributable to the partial reduction of GO to graphene. The intensity of the peak at 1628 cm^{-1} increases significantly in the CR-GO2. The presence of new peaks at 2928 and 2851 cm^{-1} are due to the adsorption of β -carotene on the surface of graphene. These observations confirm that most of the oxygen functionalities have been removed from the CR-GOs. The FT-IR spectrum of CR-GO3 is different from that of the CR-GO2. Almost all the characteristic peaks of GO are observed to be absent in the FT-IR spectrum of CR-GO3, indicating the successful reduction of GO to graphene.

3.4. Raman spectral analysis

Raman scattering is strongly dependent upon electronic structure and hence it can be useful tool to characterize graphite and graphene materials. Fig. 6 shows the Raman spectra of GO, CR-GOs, and HR-GO. Raman spectra of graphene are generally characterized by two main features: the G mode, due to the first-order scattering of E_{2g} phonons by sp^2 carbon atoms (generally observed at 1575 cm^{-1}), and the D band (1350 cm^{-1}), arising from a breathing mode of κ -point photons of A_{1g} symmetry [30,31]. In the present study, the G band of GO is broadened and shifted to 1593 cm^{-1} , while the D band is shifted to a lower region (1346 cm^{-1}) and become more prominent, indicating the destruction of sp^2 character and the formation of defects in the sheets due to extensive oxidation. The intensity ratio of the D band to the G band (I_D/I_G) of the GO is found to be ca. 0.80. In comparison to pure GO, the I_D/I_G ratios of CR-GOs increase significantly with increase in the reduction time. This is attributable to the removal of oxygen moieties and restoration of the sp^2 network during the reduction process [19,30,31]. The Raman spectrum of CR-GOs are in line with the hydrazine reduced GO reported by Stankovich et al., indicating a successful reduction process [32]. Fig. 6 also shows the Raman spectra of HR-GO to compare the quality of CR-GOs. It shows that the I_D/I_G ratio of HR-GO (1.09) is almost comparable to that of the CR-GOs indicating similar degree of defects in the reduced GO. Moreover, the G band of GO at 1593 cm^{-1} has been shifted to 1582 cm^{-1} in the CRGOs and HR-GO. This indicates that the reducing ability of carrot root is comparable to that of the hydrazine and microbial organism. Wang et al. have reported similar kind of observations in the Raman spectra of microbial reduction of graphene oxide by *Shewanella* [33]. It can also be noted that no significant change in I_D/I_G ratio has been observed with the change in temperature, suggesting that thermal treatment does not affect on the nanocrystalline nature of CR-GO [31]. The G' (2D) band of CR-GO3

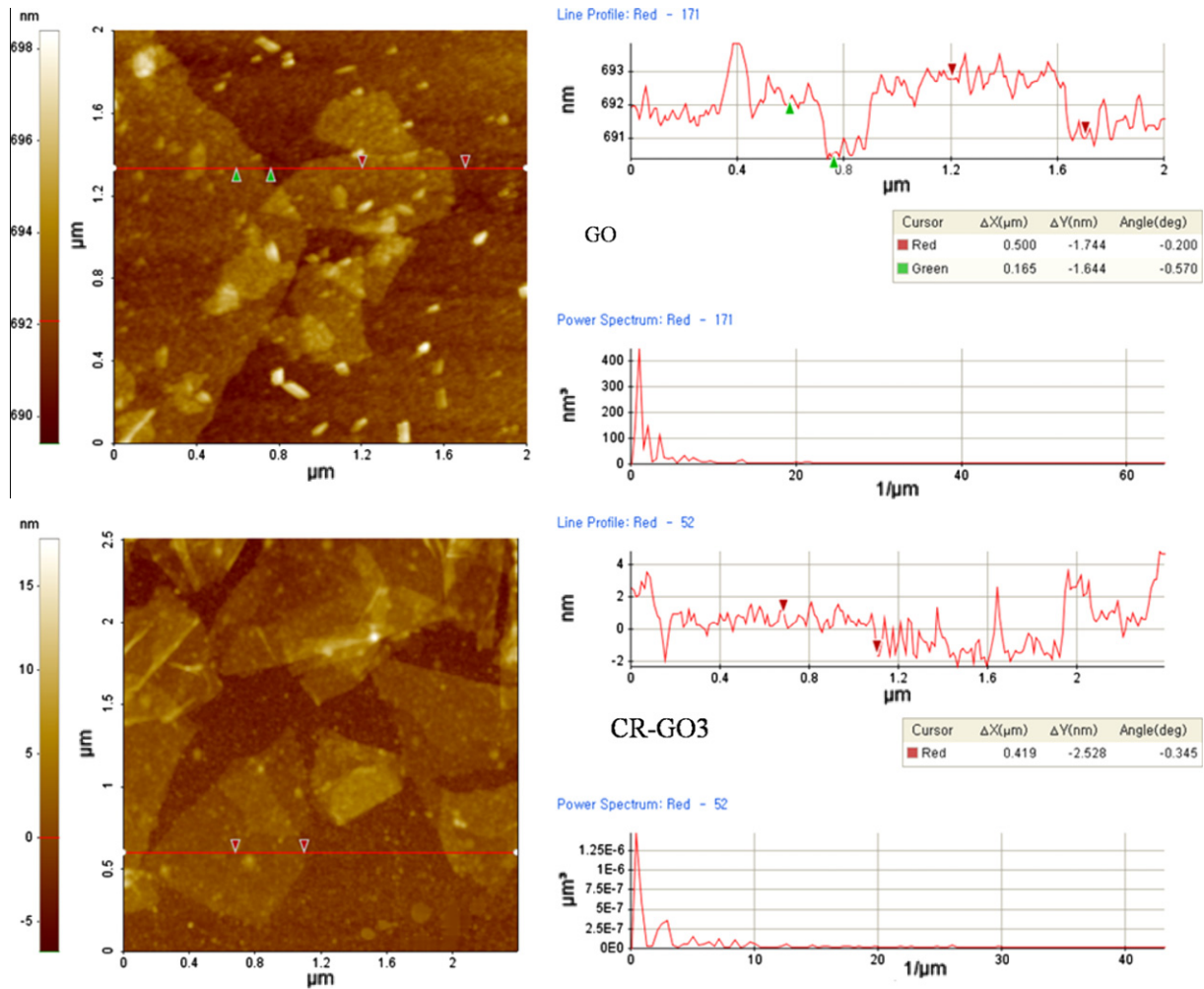


Fig. 4 – AFM images of pure GO and CR-GO3.

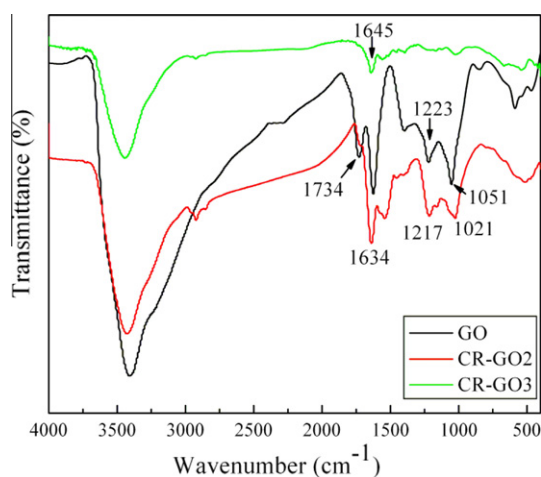


Fig. 5 – FT-IR spectra of pure GO, CR-GO2 and CR-GO3.

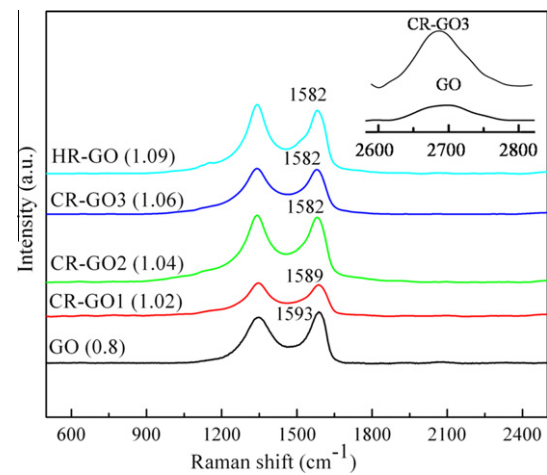


Fig. 6 – Raman spectra of pure GO, CR-GO1, CR-GO2, CR-GO3, and HR-GO.

appears at $\sim 2700\text{ cm}^{-1}$ as shown in the inset of Fig. 6. On the contrary, this band is almost absent in GO. These observations indicate the formation of graphene by the reduction of GO using wild carrot root.

3.5. XPS analysis

X-ray photoelectron spectroscopy (XPS) of pure GO, CR-GO1, CR-GO2, CR-GO3, and graphite are shown in Fig. 7a–e. The

XPS of GO shows typical C 1s peaks at 284.2, 286.4, 288.3, and 289.4 eV from sp^2 C, C–O, –C=O, and –COOH groups, respectively. The CR-GOs exhibit the same oxygen functionalities, but with greatly reduced intensities. The peak positions (G band) of CR-GOs have also been changed in comparison to pure GO. The peak shifting is attributable to the different chemical environments of C 1s carbon in the CR-GOs. The intensities of the entire C 1s peaks of carbon binding to oxygen and sp^3 carbon gradually decreases with increasing reaction time and temperature. The XPS of pure graphite shows very low intense band at 286.3 eV corresponding to C–O functionality. This is due to the aerial oxidation of graphite in air. These XPS data suggest that the oxygen-containing functional groups have been partially removed restoring majority of the conjugated graphene network after reduction [16,19,30,32]. The elemental analysis of GO, as determined by XPS, indicates the presence of 69.2% carbon and 30.1%

oxygen by atomic concentration [28]. The atomic ratios of C/O have been increased significantly in the CR-GOs as shown in Table 2.

3.6. Thermogravimetric analysis

The TGA plots of pure GO, CR-GO1, CR-GO2, and CR-GO3 are shown in Fig. 8. The TGA curve of GO shows a small mass loss (3 wt.%) at ca. 100 °C, attributable to the loss of adsorbed water from the surface of graphene. Pure GO exhibits two degradation steps; the first commencing at 165 °C, due to the loss of hydroxyl, epoxy functional groups and remaining water molecules. The second step degradation (450–600 °C) involves the pyrolysis of the remaining oxygen-containing groups as well as the burning of ring carbon [30,34,35]. In comparison to 68% weight loss at 690 °C experienced by pure GO, losses of 47%, 46%, and 21% have been noted for CR-GO1,

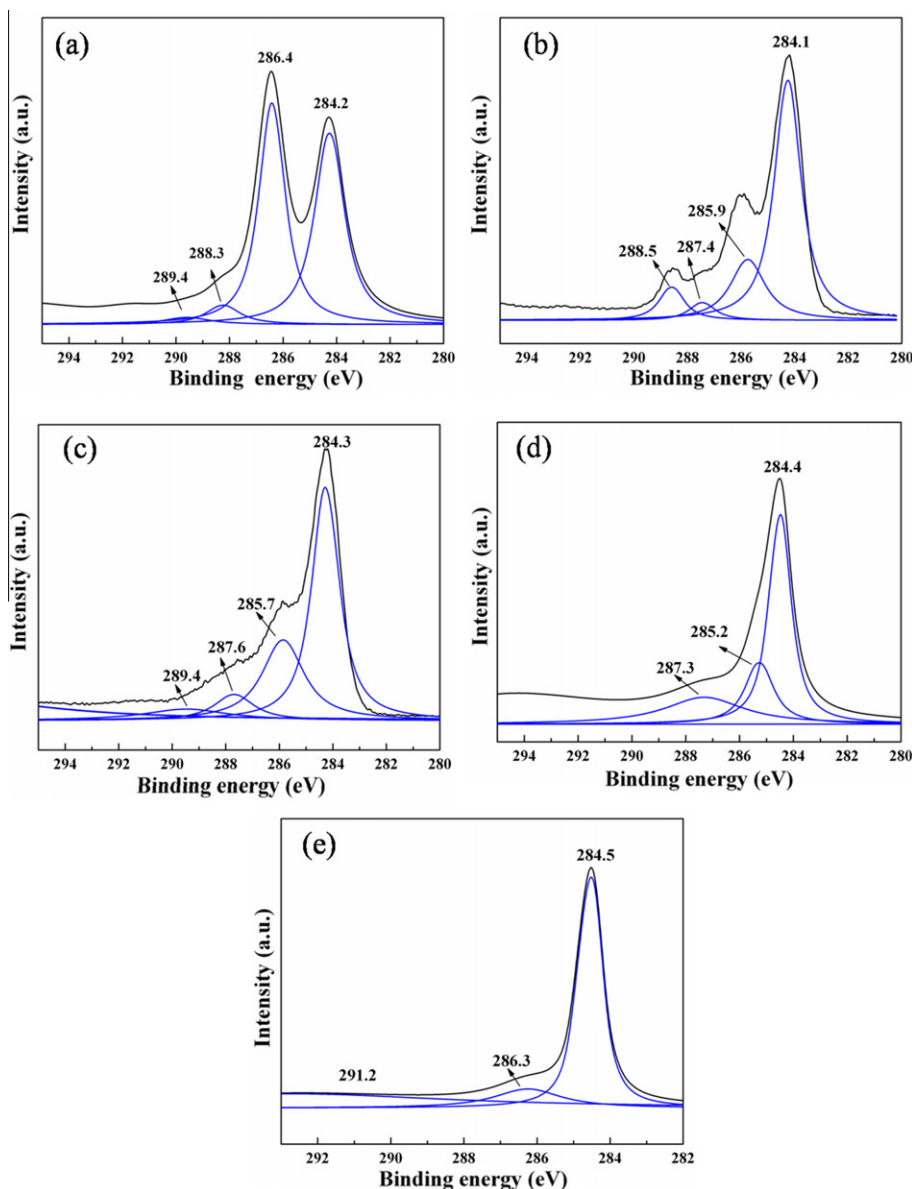
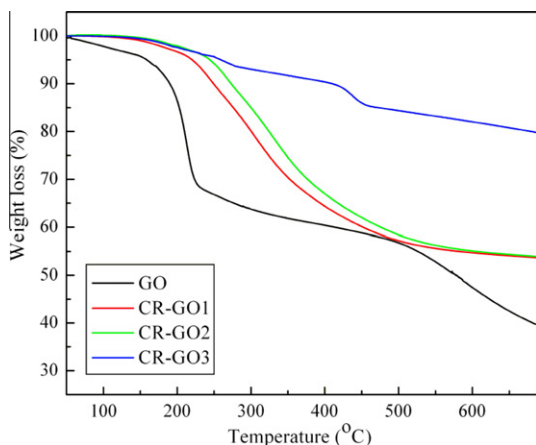


Fig. 7 – XPS of (a) pure GO, (b) CR-GO1, (c) CR-GO2, (d) CR-GO3, and (e) graphite showing the partial removal of oxygen functionalities from GO surfaces.

Table 2 – Elemental composition of GO and CR-GOs as determined by XPS.

Sample	Carbon (at.%)	Oxygen (at.%)	C/O ratio
GO	69.2	30.1	2.3
CR-GO1	81.3	18.6	4.4
CR-GO2	88.8	10.5	8.5
CR-GO3	92.1	7.7	11.9

**Fig. 8 – TGA plots of pure GO and CR-GOs.**

CR-GO2, and CR-GO3, respectively. This suggests that most of the labile oxygen functionalities have been removed from the CR-GOs. Refluxing of CR-GO is also important in aiding higher degree of reduction of GO as indicated from the lower weight loss of CR-GO3.

4. Summary

An eco-friendly and environmentally benign reduction system by using carrot root as a biocatalyst for the reduction of graphene oxide is described. The reduction was carried out in aqueous medium at room temperature. TEM and AFM reveal the formation of few layer graphene. FTIR and XPS analysis provide evidence for the elimination of labile oxygen functionality from the surface of GO. Thermal stability data of GO and CR-GO from TGA are also in line with the other experimental data. De-oxygenation and the formation of defects in the CR-GOs have been confirmed by Raman spectroscopy. The main advantages of this technique over the traditional chemical reduction are the cost-effectiveness, environmentally friendly approach and simple product isolation process.

Acknowledgement

This study was supported by the Human Resource Training Project for Regional Innovation, the Converging Research Center Program (2011K000776), and the World Class University (WCU) program (R31-20029) through the National Research

Foundation (NRF) funded by the Ministry of Education, Science, and Technology (MEST) of Korea.

REFERENCES

- [1] Novoselov KS, Geim AK, Morozov SV, Jiang D, Zhang Y, Dubonos SV, et al. Electric field effect in atomically thin carbon films. *Science* 2004;306(5696):666–9.
- [2] Geim AK. Graphene: status and prospects. *Science* 2009;324(5934):1530–4.
- [3] Zhang YB, Tan YW, Stormer HL, Kim P. Experimental observation of the quantum hall effect and berry's phase in graphene. *Nature* 2005;438:201–4.
- [4] Wu J, Pisula W, Müllen K. Graphenes as potential material for electronics. *Chem Rev* 2007;107(3):718–47.
- [5] Allen MJ, Tung VC, Kaner RB. Honeycomb Carbon: a review of graphene. *Chem Rev* 2010;110(1):132–45.
- [6] Jung JH, Cheon DS, Liu F, Lee KB, Seo TS. A graphene oxide based immune-biosensor for pathogen detection. *Angew Chem Int Ed* 2010;49(43):5708–11.
- [7] Schedin F, Geim AK, Morozov SV, Hill EW, Blake P, Katsnelson MI, et al. Detection of individual gas molecules adsorbed on graphene. *Nature* 2007;6:652–5.
- [8] Chae S, Gunes F, Kim KK, Kim ES, Han GH, Kim SM, et al. Synthesis of large-area graphene layers on poly-nickel substrate by chemical vapor deposition: wrinkle formation. *Adv Mater* 2009;21(22):2328–33.
- [9] Kim KS, Zhao Y, Jang H, Lee SY, Kim JM, Kim KS, et al. Large-scale pattern growth of graphene films for stretchable transparent electrodes. *Nature* 2009;457:706–10.
- [10] Hsia B, Ferralis N, Senesky DG, Pisano AP, Carraro C, Maboudian R. Epitaxial graphene growth on 3C-SiC(111)/AlN(0001)/Si(100). *Electrochem Solid-State Lett* 2011;14(2):k13–5.
- [11] Sun Z, Yan Z, Yao J, Beitler E, Zhu Y, Tour JM. Growth of graphene from solid carbon sources. *Nature* 2010;468:549–52.
- [12] Park S, Ruoff RS. Chemical methods for the production of graphene. *Nat Nanotechnol* 2009;4:217–24.
- [13] Si Y, Samulski T. Synthesis of water soluble graphene. *Nano Lett* 2008;8(6):1679–82.
- [14] Shan C, Yang H, Han D, Zhang Q, Ivaska A, Liu N. Water-soluble graphene covalently functionalized by biocompatible poly-L-lysine. *Langmuir* 2009;25(20):12030–3.
- [15] Bai H, Xu Y, Zhao L, Li C, Shi G. Non-covalent functionalization of graphene sheets by sulfonated polyaniline. *Chem Commun* 2009:1667–9.
- [16] Kuila T, Bose S, Hong CE, Uddin ME, Khnara P, Kim NH, et al. Preparation of functionalized graphene/linear low density polyethylene composites by a solution mixing method. *Carbon* 2011;49(3):1033–7.
- [17] Amarnath CA, Hong CE, Kim NH, Ku BC, Kuila T, Lee JH. Efficient synthesis of graphene sheets using pyrrole as a reducing agent. *Carbon* 2011;49(11):3497–502.
- [18] Dreyer DR, Murali S, Zhu Y, Ruoff RS, Bielawski CW. Reduction of graphite oxide using alcohols. *J Mater Chem* 2011;21:3443–7.
- [19] Zhang J, Yang H, Shen G, Cheng P, Zhang J, Guo S. Reduction of graphene oxide via L-ascorbic acid. *Chem Commun* 2010;46:112–4.
- [20] Salas EC, Sun Z, Luttge A, Tour JM. Reduction of graphene oxide via bacterial respiration. *ACS Nano* 2010;4(8):4852–6.
- [21] Wang Y, Shi Z, Yin J. Facile synthesis of soluble graphene via a green reduction of graphene oxide in tea Solution and its biocomposites. *Appl Mater Interface* 2011;3(4):1127–33.

- [22] Yadav JS, Nanda S, Reddy PT, Rao AB. Efficient enantioselective reduction of ketones with *Daucus carota* root. *J Org Chem* 2002;67(11):3900–3.
- [23] Caron D, Coughlan AP, Simard M, Bernier J, Piche Y, Chenevert R. Stereoselective reduction of ketones by *Daucus carota* hairy root cultures. *Biol Lett* 2005;27:713–6.
- [24] Blanchard N, Weghe PVD. *Daucus carota* L. mediated bioreduction of prochiral ketones. *Org Biomol Chem* 2006;4:2348–53.
- [25] Rodriguez P, Barton M, Aldabalde V, Onetto S, Panizza P, Menendez P, et al. Are endophytic microorganisms involved in the stereoselective reduction of ketones by *Daucus carota* root? *J Mol Catal B-Enzym* 2007;49(1–4):8–11.
- [26] Paredes JI, Villar-Rodil S, Martinez-Alonso A, Tascon JMD. Graphene oxide dispersions in organic solvents. *Langmuir* 2008;24(19):10560–4.
- [27] Hummers WS, Offeman RE. Preparation of graphitic oxide. *J Am Chem Soc* 1958;80(6):1339.
- [28] Moon IK, Lee J, Ruoff RS, Lee H. Reduced graphene oxide by chemical graphitization. *Nat Commun* 2010;1:73–8.
- [29] Hernandez Y, Nicolosi V, Lotya M, Blighe FM, Sun Z, De S, et al. High-yield production of graphene by liquid-phase exfoliation of graphite. *Nat Nanotechnol* 2008;3:563–8.
- [30] Fan ZJ, Kai W, Yan J, Wei T, Zhi LJ, Feng J, et al. Facile synthesis of graphene nanosheets via Fe reduction of exfoliated graphite oxide. *ACS Nano* 2011;5(1):191–8.
- [31] Lin Z, Yao Y, Li Z, Liu Y, Li Z, W CP. Solvent-assisted thermal reduction of graphite oxide. *J Phys Chem C* 2010;114(35):14819–25.
- [32] Stankovich S, Dikin DA, Piner RD, Kohlhaas KA, Kleinhammes A, Jia Y, et al. Synthesis of graphene-based nanosheets via chemical reduction of exfoliated graphite oxide. *Carbon* 2007;45(7):1558–65.
- [33] Wang G, Qian F, Saltikov CW, Jiao Y, Li Y. Microbial reduction of graphene oxide by shewanella. *Nano Res* 2011;4(6):563–70.
- [34] Jeong HK, Lee YP, Jin MH, Kim ES, Bae JJ, Lee YH. Thermal stability of graphite oxide. *Chem Phys Lett* 2009;470:255–8.
- [35] Chen W, Yan L, Bangal PR. Preparation of graphene by the rapid and mild thermal reduction of graphene oxide induced by microwaves. *Carbon* 2010;48(4):1146–52.